

Is one annotation enough?

A data-centric image classification benchmark for noisy and ambiguous label estimation

Lars Schmarje^{1*} Vasco Grossmann¹ Claudius Zelenka¹ Sabine Dippel² Rainer Kiko³
 Mariusz Oszust⁴ Matti Pastell⁶ Jenny Stracke⁵ Anna Valros⁶ Nina Volkmann⁷
 Reinhard Koch¹

¹MIP, Kiel University ²ITT, Friedrich-Loeffler-Institut ³LOV, Sorbonne Université
⁴Rzeszow University of Technology ⁵ITW, University Bonn ⁶University of Helsinki
⁷WING, University of Veterinary Medicine Hannover

Abstract

High-quality data is necessary for modern machine learning. However, the acquisition of such data is difficult due to noisy and ambiguous annotations of humans. The aggregation of such annotations to determine the label of an image leads to a lower data quality. We propose a data-centric image classification benchmark with nine real-world datasets and multiple annotations per image to investigate and quantify the impact of such data quality issues. We focus on a data-centric perspective by asking how we could improve the data quality. Across thousands of experiments, we show that multiple annotations allow a better approximation of the real underlying class distribution. We identify that hard labels can not capture the ambiguity of the data and this might lead to the common issue of overconfident models. Based on the presented datasets, benchmark baselines, and analysis, we create multiple research opportunities for the future.

1 Introduction

High-quality data is the fuel of modern machine learning and almost all models improve with higher quality data [5, 56, 37]. Therefore, such data are a key component for developing future techniques. The acquisition of a large amount of data is considered particularly challenging due to the participation of humans in the process. Their mistakes or subjective interpretations of annotation tasks can lead to *noisy* or *ambiguous* labels, respectively [41, 12, 44, 19, 39, 6, 13, 20]. Consequently, the labels suffer from heteroscedastic aleatoric uncertainty which means that the data contains inherent noise, which is class- or even sample-dependent and negatively affects the quality [10].

In Figure 1, we present the impact of this uncertainty on the class "cat" in the CIFAR-10 dataset [22]. While all images have the same ground truth label in CIFAR-10, humans created agreeing annotations only with varying rates from four to 100 percent [41]. This means that individual annotations can be expected to be noisy as they diverge from the majority opinion. Furthermore, a majority vote across multiple annotations can not capture the ambiguity between different images. In some extreme cases (red borders), we even see a disagreeing majority vote across all annotators from the expected ground truth class. We raise the question if all images should be treated equally if human annotations show such varying certainties. Taking a *data-centric* perspective [34, 45, 32, 17], we investigate the data in contrast to only the model for answering this question. Specifically, we propose a data-centric image classification (DCIC) benchmark that indirectly measures a method's ability to identify noisy and ambiguous labels and correct them. DCIC consists of nine real-world datasets of different domains (see Figure 2) and multiple human annotations for each image. The benchmark focuses on a

*Corresponding Author, las@informatik.uni-kiel.de

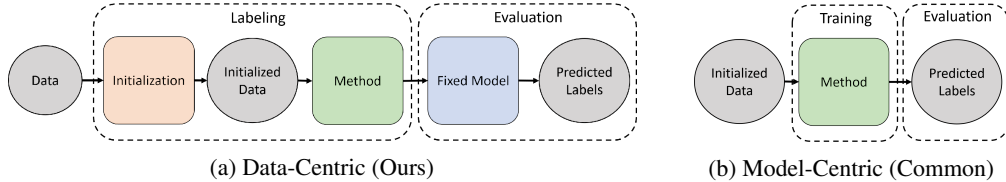


Figure 3: Comparison of our data-centric approach with the commonly used model-centric approach. There are two main differences. Firstly, we also look at how the raw unlabeled data is initialized and thus how many annotations are required. Secondly, we use a fixed model to evaluate the output of the benchmarked method. These differences lead to a greater separation of data quality and method performance on the final scores on the predicted labels.

data-centric view of the image classification problem by separating the data quality improvement and the downstream classification performance into two tasks.

The main structure of the benchmark is divided into a *Labeling* and an *Evaluation* phase (see Figure 3a). During the Labeling phase, we use samples from the distribution of the above-mentioned annotations to get different realistic label estimates as initialization for an unlabeled dataset. The initialization can be varied and describes the way the annotations are used to generate the label estimates. An initialized dataset is comparable to a predefined dataset (e.g., ImageNet [23]). The task of the benchmarked method is to improve these estimates for better performance of a downstream classification task in the second phase. In that phase (Evaluation), the obtained labels are used as input for training a fixed model and its performance is measured on a testing subset of the original data. In contrast to common model-centric deep learning approaches (see Figure 3b), we can vary the initialized dataset for the same method and better separate its performance from the data improvement. The fixed model is used for the evaluation to facilitate distinguishing between performance gains due to improved input data and better learning of the method itself.

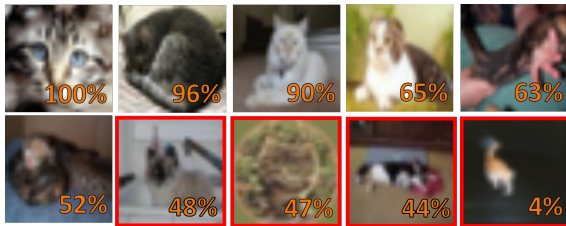


Figure 1: Are all images showing a cat? – Based on their ground truth labels from CIFAR-10 [22] they should all be cats. However, we give the agreement rate with the class cat from [41] in the lower right corner and see a wide range from four to 100%. Based on a majority vote, the last images (red border) would have not to be labeled as a cat but as dog, frog, dog, and deer, respectively. Based on these observations, we answer in our paper the question of whether all images should be treated equally as cats or if we should use multiple annotations and the resulting soft labels to capture this intrinsic noise and ambiguity.

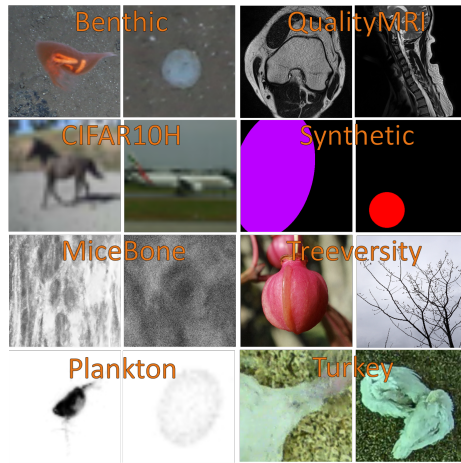


Figure 2: Two example images for all datasets. Details about the statistics of the dataset are given in Table 1.

Our benchmark is not only useful to evaluate existing methods, but will support research into algorithms for realistic datasets. We provide multiple algorithms as baselines and support the integration of more algorithms by common dataloaders for the two most popular deep learning frameworks: Tensorflow [1] and Pytorch [40]. We analyzed thousands of combinations of baseline methods, different initializations, and datasets. The obtained results confirm that the improvement of data quality leads to performance gains. Additionally, we investigated factors that influence the data quality and identified trends that lead to better learning of the underlying distribution.

Our key contributions are: (1) We collected and created nine real-world image classification datasets with multiple annotations per image. These annotations allow a realistic simulation of noise patterns

and will be helpful for future research in machine learning on real world data sets. (2) We provide a multi-domain benchmark based on these datasets for noisy and ambiguous label estimation. We implemented 20 methods as baselines. The benchmark is backend agnostic and thereby allows an easy integration of more methods from popular frameworks. (3) We conducted an analysis across various baseline methods, label initializations, and datasets. We deduce potential improvements for future annotation processes from the measured effects of the quantity and distribution of annotations during the initialization. (4) We show that one annotation per image is not enough because model performance improves as more labels are given for each input. We identify that the current focus on hard labels for classifications is ill-suited to learn the underlying ground truth distribution. A change in annotation protocols could mitigate this and lead to less overconfident models.

Related Work Data quality problems, including issues with noisy and ambiguous labels, are broadly discussed in the literature [50, 3, 41, 55, 2]. Multiple methods have been proposed, but are often evaluated on synthetic noise [31, 28]. However, Wei et al. showed that synthetic noise is different from real noise by humans, which limits the generality of findings [55]. Datasets like CIFAR-10H [41] and CIFAR-10N [55] address this issue by providing multiple annotations per image for example of the original CIFAR-10 dataset. In our benchmark, we extend this idea to eight diverse datasets apart from CIFAR-10 for a broader evaluation.

Currently, most robust methods are evaluated based on the test set accuracy [28, 50, 55, 42, 57]. However, even a small change in the structure or parameters of a method can directly impact its performance, limiting the comparability [21]. Other fields, such as Bayesian Neural Networks, address this issue by comparing results to statistical simulations, for example [18]. A recent benchmark [36] tries to overcome this issue by providing a baseline for noisy labels as a form of uncertainty estimation [10]. However, this benchmark relies on synthetic noise or noisy datasets without knowledge about the underlying ground truth distributions [29]. We use a data-centric approach to minimize the impact of implementation detail differences during the Labeling phase by evaluating on a fixed model.

2 Benchmark

Our benchmark is divided into two major phases: *Labeling* and *Evaluation*. In alignment with the Data-Centric Idea [34], we separate the improvement of the data (Labeling) from the improvement of the models (Evaluation). In general, we have an image dataset X with k known classes and use human annotations to approximate the image labels. Each image $x \in X$ has an often unknown soft ground truth label $\hat{l}_x \in [0, 1]^k$. Therefore, we use N hard human annotations $a_i \in \{0, 1\}^k$ with $i \in 1, \dots, N$ as estimates of \hat{l}_x . We assume that an average of annotations ($l_x = \sum_{i=0}^N \frac{a_i}{N}$) is an approximation of this target label \hat{l}_x as in [47]. We split the data equally and randomly in five *folds* and ensure a similar class distribution between the folds as best as possible. For one run, we use three folds as training (X_T) and one fold each as validation (X_V) and test (X_E) data, respectively. We call such a selection of folds *slice*. The benchmark can be utilized to analyze a variety of research questions, but we focus on evaluating methods that estimate noisy or ambiguous labels.

Labeling The Labeling phase consists of two steps. In the first step an initialization is used to get label estimates and in the second step, the benchmarked method Θ aims to improve these labels. As initialization, we acquire $m \in \mathbb{N}$ annotations for $n \in [0, 100]$ percent of the training and validation images. We call the total number of required annotations *budget* $b = m \cdot n$ and report it as proportions of training and validation images ($|X_T \cup X_V|$). In general, a classification task gets easier with more annotations or a higher budget. The used initialization schemes per method are defined in section 2. We chose fixed initialization schemes for better comparability between the methods. How these labels are improved by the method Θ is not restricted. However, annotations aside from the given initialization are not allowed to be used. Since we measure the quality by training a different fixed network in the next stage, a good label would be presumably as close as possible to l_x .

Evaluation In the Evaluation phase, the model and its hyperparameters are fixed to measure only the impact of the provided labels ($\Theta(x)$). The training of this fixed model Φ is calculated on the provided $\Theta(x)$ with $x \in X_T$. The best network parameters during training are selected based on a minimal divergence between $\Phi(x)$ and $\Theta(x)$ with $x \in X_V$. The generalization is then tested by measuring the difference between $\Phi(x)$ and l_x for $x \in X_E$.

Table 1: Overview of the used datasets – # is an abbreviation for number. The class imbalance is given as the percentage of the smallest and largest class with regard to the complete dataset. The agreement is the percentage of annotations that agree with the majority vote. The scores ACC and \hat{ACC} are given for the supervised baseline across three test folds. The access describes if the (raw) data is available openly, requires permission (restricted) or was not previously available (N/A). In the last column, datasets with modifications to the original data are marked with X. A modification might be adding more annotations or crop images to a region of interest.

Name	# classes	Input size [px]	# Images	Class Imbalance [%]		Agreement [%] Mean \pm STD	# Annotations Mean \pm STD	ACC [%] Mean \pm STD	\hat{ACC} [%] Mean \pm STD	Access	Updated
				Smallest	Largest						
Benthic	10	112 \times 112	4867	2.31	39.66	82.61 \pm 19.67	4.54 \pm 2.01	64.17 \pm 0.63	83.36 \pm 0.47	Restricted	X
CIFAR-10H	10	32 \times 32	10000	9.88	10.16	95.44 \pm 8.91	51.10 \pm 1.54	90.75 \pm 0.39	95.72 \pm 0.12	Open	
Mice Bone	3	224 \times 224	7240	14.75	70.48	85.06 \pm 17.52	15.30 \pm 21.90	61.88 \pm 9.44	78.39 \pm 1.95	Restricted	X
Plankton	10	96 \times 96	12280	4.16	30.37	93.26 \pm 13.60	24.38 \pm 44.17	89.89 \pm 0.82	92.41 \pm 0.41	Restricted	
Quality MRI	2	224 \times 224	310	34.84	64.16	71.56 \pm 12.27	99.94 \pm 13.44	66.62 \pm 3.55	75.81 \pm 0.17	Restricted	X
Synthetic	6	224 \times 224	15000	16.17	17.57	74.41 \pm 24.28	98.86 \pm 0.99	87.85 \pm 0.48	74.65 \pm 0.34	N/A	X
Treeversity#1	6	224 \times 224	9489	9.98	30.67	88.60 \pm 16.13	14.78 \pm 7.06	79.50 \pm 1.53	89.20 \pm 0.31	Open	X
Treeversity#6	6	224 \times 224	9826	8.77	31.26	66.53 \pm 19.48	35.45 \pm 11.47	56.71 \pm 4.89	68.88 \pm 0.72	Open	X
Turkey	3	192 \times 192	8040	10.88	75.95	91.56 \pm 13.82	14.85 \pm 20.95	75.51 \pm 2.80	86.89 \pm 1.03	Restricted	X

Metrics Kullback-Leibler divergence (KL) [24] between $\Phi(x)$ and l_x for $x \in X_E$ has been used as our main metric since it measures the difference between two distributions [35]. To ensure a high reproducibility, we averaged in a 3-fold cross-validation per dataset. We used the three slices defined by $X_{V_i} = \{f_{i+1}\}$, $X_{E_i} = \{f_{i+2}\}$ and the rest as training for the folds f_1, \dots, f_5 , $i \in 1, 2, 3$. Additionally, we evaluate the accuracy (ACC) and F1-Score ($F1$) between $\Phi(x)$ and l_x for $x \in X_E$ per class and report the mean across the classes, which is commonly called the macro value. Without the macro averaging, the class imbalance would impair the interpretability of the results. We analyze the calibration of the trained models by reporting the Expected Calibration Error (ECE) [16]. As reference, we provide all of these metrics also on the difference between $\Theta(x)$ and l_x for $x \in X_E$. The metrics are noted as \hat{ACC} , $\hat{F1}$ and \hat{ECE} . Also, we report the Cohen’s Kappa Score (κ) [33] as the measurement of the consistency of $\Theta(x)$ between the folds under the assumption that more consistent labels result in higher model performance.

Datasets We include nine real-world classification datasets in our benchmark. Since we need multiple annotations per image for the evaluation of the quality of labels and this information is often not available in existing datasets or insufficient for our benchmark, we collected, adopted, or extended annotations of the following datasets. Their details are shortly described below, while their properties and exemplary images are shown in Table 1 and Figure 2, respectively. As presented, the datasets vary across all reported properties, giving an opportunity to comprehensively evaluate considered methods. More challenging datasets are characterized by a high-class imbalance, a low average agreement, or a low number of annotations per image. Detailed reports about the collection process and remaining dataset specifics are given in the supplementary.

1. *Benthic* depicts images from the seafloor and consists of underwater flora and fauna. We used annotations from [48, 26] but filtered for at least three annotations per object and cropped the main image to this object. We combined classes with too few images in agreement with domain experts. 2. *CIFAR-10H* is a variant of CIFAR-10 [22] introduced in [41]. Peterson et al. analyzed the underlying class distribution like us by reannotating the CIFAR-10 test set. In contrast to other variants like CIFAR-10N [55], this dataset provides more annotations per image. 3. *MiceBone* consists of Second-Harmonic-Generation images of collagen fibers in mice [43]. The raw images were preprocessed as described in [47]. Since there is a need for multiple annotations per image, we hired workers to increase their number by a factor of five. 4. *Plankton* is a collection of underwater plankton images with multiple annotations from citizen scientists [44]. We use the preprocessing described in [47]. 5. *QualityMRI* consists of human magnetic resonance images (MRI) with a varying quality and multiple subjective quality ratings gathered in tests with radiologists. It was introduced and evaluated in [38, 51]. 6. *Synthetic* dataset was generated for the purpose of this study. It consists of images that contain one blue, red, or green circle or ellipse on a black background. To create ambiguous images, we added color and axis interpolations of these classes. 7+8. *TreeVersity* is a publicly available crowdsourced dataset of plant images from the Arnold Arboretum of Harvard University². In the crowdsourcing project, the images were tagged with a given set of labels. We used a simplified version with six classes where we combined classes with too few images. Only images with at least

²<https://arboretum.harvard.edu/research/data-resources/>

Table 2: Overview of used methods grouped into supervised, semi-supervised and self-supervised. The second to fifth column describe if the method uses unlabeled data, makes noise estimation, what pretraining is the used input of the initialized dataset are hard or soft labels, respectively. The initialization schemes columns describe which schemes were evaluated for individual methods. The average runtime of the labeling phase is given in the last column.

Name	Unlabeled Data	Noise Estimation	Pretraining	Labels	Initialization Schemes				Avg. Runtime [h]
					SL	SL+	SSL	SSL+	
Baseline				Soft	X	X	X	X	0.00
Heteroscedastic (Het) [11]		X		Hard	X	X	X	X	0.50
SNGP [30]		X		Hard	X	X	X	X	0.29
ELR+ [31]		X	ImageNet	Hard	X	X	X	X	0.09
Mean-Teacher (Mean) [52]	X			Hard	X		X		1.08
Mean-Teacher (Mean+DC3) [47]	X			Hard	X		X		1.20
π -Model (π) [25]	X			Hard	X		X		1.03
π -Model (π +DC3) [47]	X			Hard	X		X		1.15
FixMatch [49]	X			Hard	X		X		4.53
FixMatch+DC3 [47]	X			Hard	X		X		4.01
Pseudo-Label (Pseudo v1) [27]	X			Hard	X		X		1.10
Pseudo-Label (Pseudo v1 +DC3) [47]	X			Hard	X		X		1.40
Pseudo-Label (Pseudo v2 hard) [27]	X		ImageNet	Hard	X	X	X	X	0.16
Pseudo-Label (Pseudo v2 soft) [27]	X		ImageNet	Soft	X	X	X	X	0.12
Pseudo-Label (Pseudo v2 not) [27]	X			Soft	X	X	X	X	0.12
DivideMix [28]	X	X	ImageNet	Hard	X	X	X	X	1.39
BYOL [15]	X		Self-Supervised	Hard	X		X		2.59
MOCOv2 [9]	X		Self-Supervised	Hard	X		X		7.94
SimCLR [8]	X		Self-Supervised	Hard	X		X		5.89
SWAV [7]	X		Self-Supervised	Hard	X		X		4.17

three tags were used. Tags are not the same as class labels, therefore, we provide two subsets of TreeVersity. In TreeVersity#1, we filtered for exactly one given tag of the six possible ones per user which is similar to a classification. In TreeVersity#6, we filtered for a maximum of six different tags which means we did not apply any restrictions. 9. *Turkey* is a dataset with images of turkeys and their injuries [54, 53]. We used the preprocessing described in [47] and extended the original annotations, increasing their number by a factor of five with hired workers.

Methods We compare a variety of recent supervised, self-supervised, and semi-supervised algorithms against our baseline, a supervised training with a cross-entropy loss. The *supervised* methods are Heteroscedastic [11], SNGP [30], and ELR+ [31]. The *semi-supervised* methods are Mean-Teacher [52], π -Model [25], FixMatch [49], DC3 [47], Pseudo-Label [27], and DivideMix [28]. The *self-supervised* methods are BYOL [15], MOCOv2 [9], SimCLR [8], and SWAV [7]. Detailed descriptions about most of them are given in [46] and their key characteristics are presented in Table 2. We use the reported hyperparameters for Imagenet [23] or Webvision [29] by the original authors to ensure a comparison out-of-the-box across different image domains. For DC3[47], we investigated the combinations with Mean-Teacher, π -Model, FixMatch, and Pseudo-Label. For Pseudo-Label, we used two different implementations (v1 and v2) and variants with or without pretraining and soft or hard labels as input. In total, this results in 20 investigated methods. For better referencing, we group them as described above but put methods that *use soft labels* into their own group.

Initialization Schemes We investigated a fixed set of initialization schemes and note them m - n for m annotations for a subset of data with a relative size n . For easier reference, we group them as

- *Supervised Learning (SL)* 01-1.00
- *Supervised Learning+ (SL+)* 03-1.00, 05-1.00, 10-1.00
- *Semi-Supervised Learning (SSL)* 01-0.10, 01-0.20, 01-0.50
- *Semi-Supervised Learning (SSL+)* 10-0.10, 05-0.20, 02-0.50

Implementation Details The final results depend on a good set of fixed hyperparameters like learning rate or batch size for the model Φ for each dataset during the evaluation. Therefore, we determined them by applying Hyperopt [4] with 100 search trials across the same grid of parameters for all datasets. The target was the minimization of KL between $\Phi(x)$ and l_x for the baseline experiment with exactly ten annotations per image across one slice. We executed these and later experiments on an Nvidia RTX 3090 with 24GB VRAM or comparable hardware. Some combinations

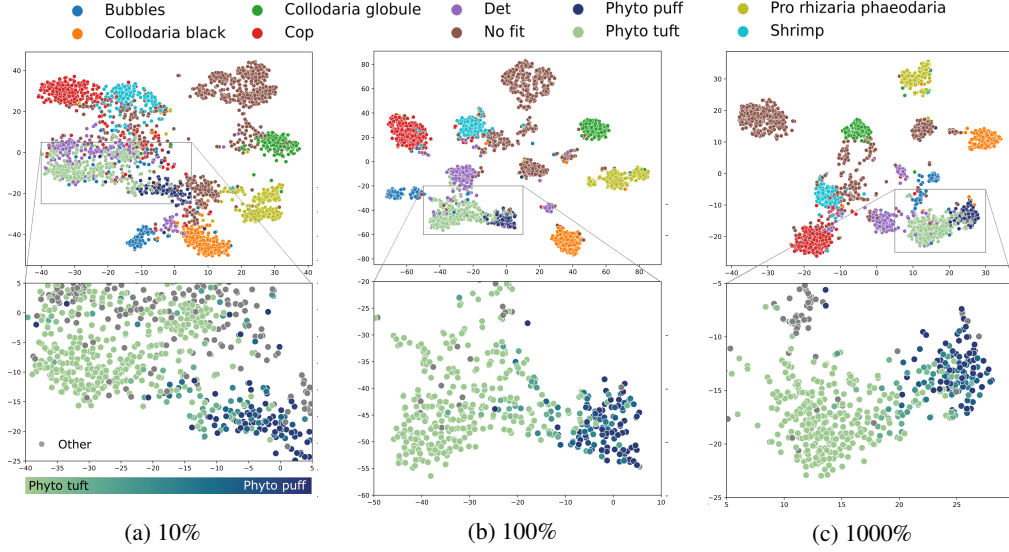


Figure 4: T-SNE evaluation on Plankton dataset on a budget of 10%, 100% and 1000% – On the top, all images are colored based on the majority class of the ground truth distribution. The lower images are zoomed in regions where we color only two classes accordingly to their actual ground truth distribution.

of models and input sizes could not fit on this hardware and therefore were ignored to keep the needed hardware to a minimum. Details about the used parameter grid are given in the supplementary. We ensure that all folds are randomly generated, while restrictions about similar images are considered. Without these restrictions, similar images, e.g., frames from the same camera might lead to an information leakage between the folds which would negatively influence the interpretability of the results.

3 Analysis

The evaluation was conducted across combinations of all datasets, methods, initialization schemes, and slices. A complete cross-combination would result in 5400 experiments from which we selected 3456 experiments to save resources since some combinations would not add more insights. A detailed overview of the initialization schemes used per method can be found in Table 2. As shown in Table 1, we have a large variability between the datasets, especially in ACC and \hat{ACC} that range from 57% to 96%. The datasets Benthic, MiceBone, Treeversity#6, and Turkey have an over 10% lower ACC than the expected \hat{ACC} , which marks them as particularly challenging for the model. Moreover, the datasets Benthic, MiceBone, QualitMRI, and Treeversity#6 have an \hat{ACC} of lower than 80% which marks them as difficult even for humans. Thus, we call them *difficult* and the rest *easy* datasets. The \hat{ACC} of Synthetic is even lower due to the artificially created labels. Due to this variability, an average across the scores can be misleading. For this reason, we report the median in this paper and report the full results including the standard error of the mean (SEM) in the supplementary.

More annotations are better It is to be expected that more and better data should lead to increased performance which we quantify in Figure 5a. It can be seen that all metrics improve with an increased budget in the form of more annotated data or more annotations per image. However, the impact is lower for more annotations per image. For example, ACC increases from around 58% to 71% for the full supervision. Up to 10 annotations per image increase the score only to around 77%. This difference can be explained by the fact that additional annotations are most valuable to improve uncertain labels. For easier datasets, we see in Figure 5b that the improvements with additional annotations are lower or do not exist, supporting the observation above. If we check in Figure 5c which methods benefit the most from additional annotations, we see up to 0.15 lower relative KL and ECE for soft labels. We can confirm similar observations on a t-SNE [14] visualization of the Plankton dataset in Figure 4. For a budget of 10%, the clusters are not as distinct as with 100% while

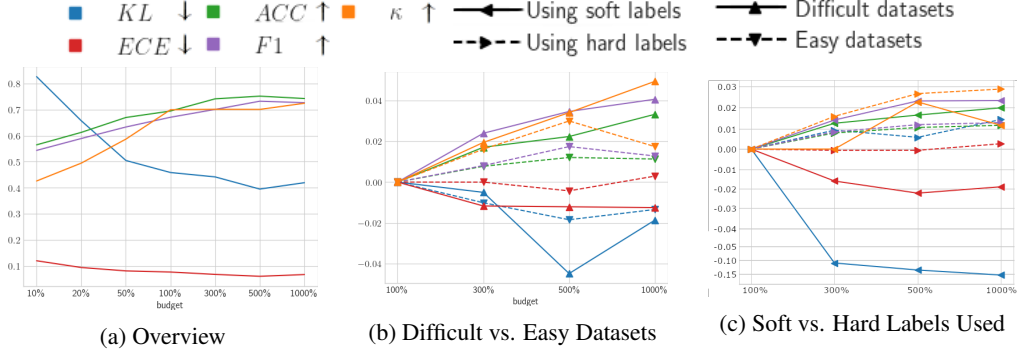


Figure 5: Impact of increased budget across all methods and datasets – The last two images show the relative changes in comparison to a budget of 100% from different subgroups of the datasets and methods respectively.

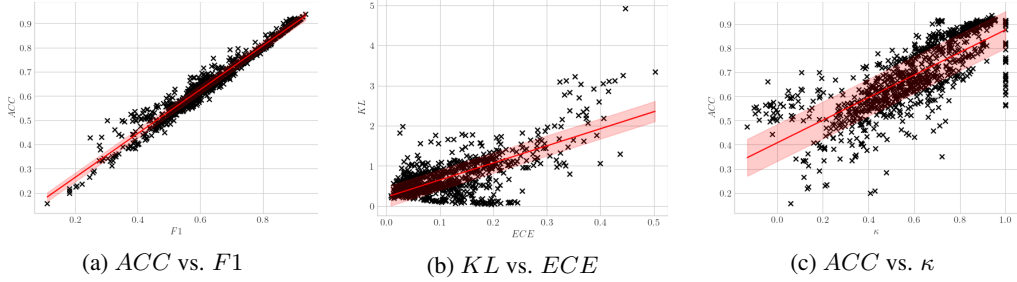


Figure 6: Correlations between selected metrics across all experiments. The red line represents the linear regression between the metrics and the light red area the mean absolute error of the regression.

for a budget of 1000% we can see more linear transitions in alignment with the soft ground truth label.

Correlations and their implications We analyzed the correlations between our metrics to determine which contain the same or similar information and which are complementary. All calculated Pearson correlation coefficients have a p-value < 0.01 and the four strongest correlations are ACC vs. $F1$ (0.98), KL vs. ECE (0.70), $F1$ vs. κ (0.78) and ACC vs. κ (0.77) (partially shown in Figure 6). The other correlations are around -0.5. $F1$ balances the precision and recall but in our experiments we see almost identical values to ACC which we credit to the averaging per class. A high correlation also exists between ACC and κ which means that higher consistency in the input labels for different folds leads to better classification scores. This is a particularly useful result since consistency can be calculated without training a network or knowing anything about the ground truth distribution. Overconfident models are a problem of modern machine learning [16] and the higher correlation between KL and ECE compared to any of the two with ACC , $F1$ or κ indicates that our focus on classification metrics like ACC and $F1$ could be the issue.

The benefit of knowledge transfer In Figure 7a, we present the impact on KL , ACC , and ECE due to the additional training of a fixed model in our data-centric approach. We see that KL is about half as small as \hat{KL} , ECE is around 3-5% lower than \hat{ECE} and ACC is 1-2% better than \hat{ACC} if we consider the mean and the other way round if we consider the median. We conclude that the impact of a second training on the soft output predictions for ACC is minimal while it leads to a reduction in KL and ECE .

Quantity vs. Quality While a higher budget leads to improved metrics, it also matters how it is used. In Figure 7b, we investigated the impact on KL and ACC for a budget of 100% for Pseudo-Label using hard or soft labels. We find that the accuracy is comparable between the methods and increases with a rising percentage of labeled data (m). For hard labels, the KL improves equally.

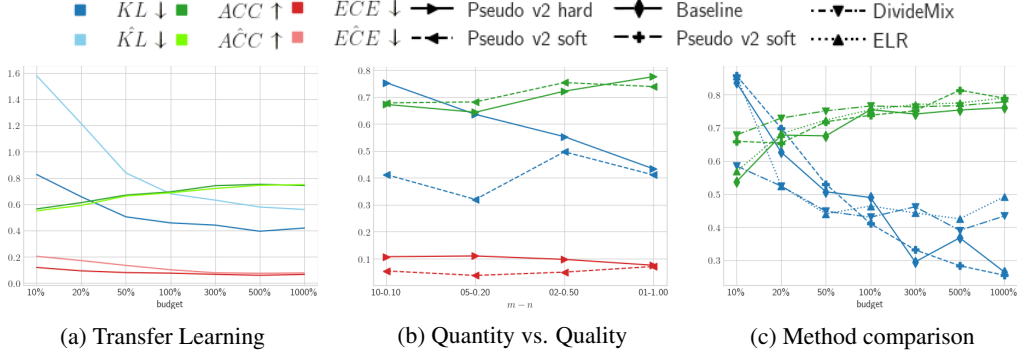


Figure 7: Analysis of all or selected methods across different budgets or initialization schemes.

Table 3: Results for the best performing methods – The best metric is marked bold while the 2nd and 3rd best are italic. Only methods with at least one top3 ranking across the budgets are presented. The full results are in the supplementary. (a) show the relative improvement over the baseline. (b) are detailed results for the budget of 100% across all datasets.

(a) Improvements						(b) Details 100% Budget										
Budget	10%		100%		1000%		Dataset	Benthic	CIFAR10H	MiceBone	Plankton	QualityMRI	Synthetic	Treeversity#1	Treeversity#6	Turkey
	Median	Mean \pm SEM	Median	Mean \pm SEM	Median	Mean \pm SEM	Baseline	1.17 \pm 0.04	0.41 \pm 0.02	0.55 \pm 0.06	0.34 \pm 0.02	1.73 \pm 0.48	0.08 \pm 0.01	0.49 \pm 0.04	1.02 \pm 0.03	0.40 \pm 0.08
ELR+	-0.13	-0.63 \pm 0.25	-0.12	-0.18 \pm 0.07	0.11	0.25 \pm 0.07	ELR+	0.70 \pm 0.01	0.29 \pm 0.02	0.29 \pm 0.01	0.24 \pm 0.03	1.44 \pm 0.83	0.18 \pm 0.02	0.46 \pm 0.01	0.47 \pm 0.05	0.52 \pm 0.05
SGNP	-0.30	-0.63 \pm 0.30	-0.01	-0.17 \pm 0.09	0.17	0.23 \pm 0.04	SGNP	1.11 \pm 0.05	0.38 \pm 0.01	0.56 \pm 0.14	0.33 \pm 0.02	0.25 \pm 0.14	0.10 \pm 0.00	0.46 \pm 0.01	1.07 \pm 0.05	0.42 \pm 0.08
DivideMix	-0.31	-0.86 \pm 0.28	-0.05	-0.21 \pm 0.08	0.14	0.29 \pm 0.08	DivideMix	0.87 \pm 0.07	0.36 \pm 0.02	0.38 \pm 0.05	0.34 \pm 0.01	0.46 \pm 0.26	0.33 \pm 0.00	0.47 \pm 0.01	0.62 \pm 0.05	0.43 \pm 0.08
Mean	-0.14	-0.66 \pm 0.24	-0.13	-0.23 \pm 0.09	N/A	N/A	Mean	0.80 \pm 0.06	0.28 \pm 0.02	0.38 \pm 0.02	0.32 \pm 0.01	0.35 \pm 0.11	0.09 \pm 0.01	0.61 \pm 0.01	0.52 \pm 0.03	0.75 \pm 0.07
Mean+DC3	-0.23	-0.55 \pm 0.18	-0.12	-0.16 \pm 0.07	N/A	N/A	Mean+DC3	0.73 \pm 0.02	0.28 \pm 0.04	0.37 \pm 0.00	0.30 \pm 0.02	1.42 \pm 0.93	0.11 \pm 0.02	0.51 \pm 0.01	0.48 \pm 0.02	0.55 \pm 0.10
π	-0.34	-0.69 \pm 0.21	-0.08	-0.20 \pm 0.06	N/A	N/A	π	0.71 \pm 0.03	0.33 \pm 0.02	0.38 \pm 0.00	0.30 \pm 0.02	0.98 \pm 0.04	0.08 \pm 0.01	0.52 \pm 0.01	0.51 \pm 0.03	0.55 \pm 0.01
π +DC3	-0.36	-0.67 \pm 0.22	-0.11	-0.23 \pm 0.06	N/A	N/A	π +DC3	0.72 \pm 0.06	0.30 \pm 0.02	0.39 \pm 0.04	0.29 \pm 0.01	0.88 \pm 0.34	0.08 \pm 0.00	0.48 \pm 0.01	0.49 \pm 0.00	0.44 \pm 0.08
Pseudo v2 soft	-0.37	-0.43 \pm 0.21	-0.03	-0.19 \pm 0.07	0.01	-0.00 \pm 0.02	Pseudo v2 soft	1.00 \pm 0.08	0.41 \pm 0.02	0.40 \pm 0.08	0.32 \pm 0.06	0.62 \pm 0.16	0.10 \pm 0.01	0.46 \pm 0.01	0.83 \pm 0.13	0.37 \pm 0.08
MOCOv2	-0.36	-0.68 \pm 0.24	0.02	-0.13 \pm 0.11	N/A	N/A	MOCOv2	0.91 \pm 0.05	0.98 \pm 0.02	0.37 \pm 0.04	0.52 \pm 0.01	0.29 \pm 0.11	0.13 \pm 0.01	0.80 \pm 0.03	0.61 \pm 0.01	0.42 \pm 0.08

If we use soft labels for training, we see lower results for 05-0.20 and 02-0.50. We conclude that it is not optimal for all datasets to annotate the complete data if we are interested in the ground truth distribution.

State-of-the-art comparison To determine the best-performing state-of-the-art method, we gathered their relative improvements over the baseline in Table 3a. The best algorithm for each type of the soft, semi-supervised, supervised, self-supervised approach based on the average performance across the budgets of 10%, 100%, and 1000% are Pseudo v2 soft, DivideMix, ELR+, and Mocov2, respectively. We visualize the best three of them in Figure 7c and give detailed results across the datasets for the budget 100% in Table 3b. The full results can be found in the supplementary. All top three methods are pretrained on ImageNet and outperform the rest in the field they were designed for. DivideMix is the best during partial supervision (budget < 100%), ELR+ is more noise robust (budget > 100%), and Pseudo v2 soft has the lowest KL score (budget > 100%). However, we cannot identify a superior approach across all domains and the baseline is the best method for 1000%. Moreover, an average better performance does not mean that the gains are equal across all datasets. For example, ELR+ has the lowest KL at a budget of 100% for five out of nine datasets but on the QualityMRI dataset, it is among the worst methods.

4 Discussion

Overall, we can demonstrate that data quality positively impacts the classifications scores like ACC and $F1$ and distribution-based scores like KL and ECE . Additionally, KL and ECE are highly correlated (0.7) and are improved more when using soft labels. Hence, we believe that focusing on learning the real distribution and thus minimizing KL can lead to less overconfident models. Using soft labels as input seems to be crucial for achieving this since hard labels and classification metrics like ACC lead to models which slightly ignore the real ground truth distribution. Additionally, we showed that it can be beneficial to annotate some images multiple times instead of all images once.

Impact This work as a benchmark provides nine datasets and a detailed evaluation across 20 algorithms on this benchmark. The provided data can allow the investigation of research questions

on the topics of e.g. noise estimation, data annotation scheme, or realistic semi-supervised learning. The analysis shows a rather large gap between the current common goal ACC and understanding and predicting the real ground truth distribution. This work is intended to allow and spark future research and thus no direct social impacts are expected. However, this basic research is time and resource-consuming. For the final evaluation, we conducted experiments with about 5500 GPU hours which equals around 600kg CO_2 . For this reason, we limited the evaluation always to necessary elements when possible in order to not increase the needed GPU hours further.

Limitations The 20 investigated algorithms are only evaluated with one fixed set of hyperparameters across different datasets during the labeling phase. For optimal performance, a tuning per algorithm would have been required. We were interested in the general performance out-of-the-box and therefore neglected this issue due to resource minimization. The researched datasets are all below 15,000 images and the unsupervised learning potential on millions of images could not be investigated. We want to provide a detailed analysis in relation to the underlying distribution l_x per image which is only possible with multiple annotations per image. For larger datasets, this effort was just not feasible. As described above we conducted more than a thousand experiments but we had to select and combine several results in a comprehensive manner in this paper. These aggregations can not capture all details. Much more detailed analysis e.g., per dataset would be possible and thus we included all raw results in the supplementary. Due to the fixed initialization scheme, we can not investigate active learning approaches. However, this restriction is chosen to allow a better comparability and future researchers could decide against such a restriction.

Conclusion We provide a wide-ranged realistic benchmark with nine datasets and 20 baselines. On this benchmark, we conducted a detailed analysis and identified the benefits of multiple annotations per image. Moreover, we conclude that hard labels are well suited for improving classification scores like ACC but should be replaced with soft labels to learn the real underlying distribution. These changes could also minimize side effects like overconfident models. We identify several research opportunities with soft labels, provide all raw analysis results for the investigation of other research questions and the datasets could even be used to research other topics like active learning.

Acknowledgments and Disclosure of Funding

We thank Mark Collier for his valuable feedback and discussion about the benchmark.

We acknowledge funding of L. Schmarje by the ARTEMIS project (Grant number 01EC1908E) funded by the Federal Ministry of Education and Research (BMBF, Germany). R. Kiko also acknowledges support via a “Make Our Planet Great Again” grant of the French National Research Agency within the “Programme d’Investissements d’Avenir”; reference “ANR-19-MPGA-0012”. V. Grossmann is employed with funds provided by Kiel Marine Science (KMS) and Future Ocean Network (FON) by Kiel University. Funds to conduct the PlanktonID project were granted to R. Kiko and R. Koch (CP1733) by the Cluster of Excellence 80 “Future Ocean” within the framework of the Excellence Initiative by the Deutsche Forschungsgemeinschaft (DFG) on behalf of the German federal and state governments. Turkey data set was collected as part of the project “RedAlert – detection of pecking injuries in turkeys using neural networks” which was supported by the “Animal Welfare Innovation Award” of the “Initiative Tierwohl”.

References

- [1] Martin Abadi, Paul Barham, Jianmin Chen, Zhifeng Chen, Andy Davis, Jeffrey Dean, Matthieu Devin, Sanjay Ghemawat, Geoffrey Irving, Michael Isard, Manjunath Kudler, Josh Levensberg, Rajat Monga, Sherry Moore, Derek Murray, Benoit Steiner, Paul Tucker, Vijay Vasudevan, Pete Warden, Martin Wicke, Yuan Yu, and Xiaoqiang Zheng. TensorFlow: A System for Large-Scale Machine Learning. In *12th USENIX symposium on operating systems design and implementation (OSDI 16)*, pages 265–283, 2016.
- [2] P. F.E. E E Addison, D. J. Collins, R. Trebilco, S. Howe, N. Bax, P. Hedge, G. Jones, P. Miloslavich, C. Roelfsema, M. Sams, R. D. Stuart-Smith, P. Scanes, P. Von Baumgarten, and A. McQuatters-Gollop. A new wave of marine evidence-based management: Emerging

- challenges and solutions to transform monitoring, evaluating, and reporting. *ICES Journal of Marine Science*, 75(3):941–952, 2018. ISSN 10959289. doi: 10.1093/icesjms/fsx216.
- [3] Görkem Algan and Ilkay Ulusoy. Image Classification with Deep Learning in the Presence of Noisy Labels: A Survey. *Knowledge-Based Systems*, 2020. ISSN 23318422. doi: 10.1016/j.knosys.2021.106771.
 - [4] James Bergstra, Daniel Yamins, and David Cox. Making a science of model search: Hyperparameter optimization in hundreds of dimensions for vision architectures. In *International conference on machine learning*, pages 115–123. PMLR, 2013.
 - [5] Lucas Beyer, Olivier J. Hénaff, Alexander Kolesnikov, Xiaohua Zhai, Aäron van den Oord, Aäron van den Oord, and Aäron van den Oord. Are we done with ImageNet? *arXiv preprint arXiv:2006.07159*, 2020.
 - [6] J Brünger, S Dippel, R Koch, and C Veit. ‘Tailception’: using neural networks for assessing tail lesions on pictures of pig carcasses. *Animal*, 13(5):1030–1036, 2019. ISSN 17517311. doi: 10.1017/S1751731118003038.
 - [7] Mathilde Caron, Priya Goyal, Ishan Misra, Piotr Bojanowski, Julien Mairal, and Armand Joulin. Unsupervised Learning of Visual Features by Contrasting Cluster Assignments. *Proceedings of Advances in Neural Information Processing Systems (NeurIPS)*, 2020. ISSN 23318422.
 - [8] Ting Chen, Simon Kornblith, Mohammad Norouzi, and Geoffrey Hinton. A Simple Framework for Contrastive Learning of Visual Representations. *arXiv preprint arXiv:2002.05709*, (PMLR): 1597–1607, 2020. ISSN 23318422.
 - [9] Xinlei Chen, Haoqi Fan, Ross Girshick, and Kaiming He. Improved Baselines with Momentum Contrastive Learning. *arXiv preprint arXiv:2003.04297*, 2020.
 - [10] Mark Collier, Basil Mustafa, Efi Kokiopoulou, Rodolphe Jenatton, and Jesse Berent. A Simple Probabilistic Method for Deep Classification under Input-Dependent Label Noise. *arXiv preprint arXiv:2003.06778*, 2020.
 - [11] Mark Collier, Basil Mustafa, Efi Kokiopoulou, Rodolphe Jenatton, and Jesse Berent. Correlated Input-Dependent Label Noise in Large-Scale Image Classification. *Proceedings of the IEEE/CVF Conference on Computer Vision and Pattern Recognition*, (c):1551–1560, 2021.
 - [12] Phil Culverhouse, Robert Williams, Beatriz Reguera, Vincent Herry, and Sonsoles González-Gil. Do experts make mistakes? A comparison of human and machine identification of dinoflagellates. *Marine Ecology Progress Series*, 247:17–25, 2003. doi: 10.3354/meps247017.
 - [13] Jeffrey De Fauw, Joseph R Ledsam, Bernardino Romera-Paredes, Stanislav Nikolov, Nenad Tomasev, Sam Blackwell, Harry Askham, Xavier Glorot, Brendan O’Donoghue, Daniel Visentin, Others, Brendan O’Donoghue, Daniel Visentin, and Others. Clinically applicable deep learning for diagnosis and referral in retinal disease. *Nature medicine*, 24(9):1342–1350, 2018.
 - [14] Laurens der Maaten and Geoffrey Hinton. Visualizing data using t-SNE. *Journal of machine learning research*, 9(11), 2008.
 - [15] Jean-Bastien Grill, Florian Strub, Florent Altché, Corentin Tallec, Pierre H. Richemond, Elena Buchatskaya, Carl Doersch, Bernardo Avila Pires, Zhaohan Daniel Guo, Mohammad Gheshlaghi Azar, Bilal Piot, Koray Kavukcuoglu, Rémi Munos, and Michal Valko. Bootstrap your own latent: A new approach to self-supervised Learning. *Advances in Neural Information Processing Systems 33 pre-proceedings (NeurIPS 2020)*, 2020.
 - [16] Chuan Guo, Geoff Pleiss, Yu Sun, and Kilian Q Weinberger. On calibration of modern neural networks. In *International Conference on Machine Learning*, pages 1321–1330. PMLR, 2017.
 - [17] Tony Hey. The Fourth Paradigm – Data-Intensive Scientific Discovery. In *Communications in Computer and Information Science*, pages 1–1. 2012. doi: 10.1007/978-3-642-33299-9_1.
 - [18] Pavel Izmailov, Sharad Vikram, Matthew D. Hoffman, and Andrew Gordon Gordon Wilson. What Are Bayesian Neural Network Posteriors Really Like? *International Conference on Machine Learning*, pages 4629–4640, 2021.

- [19] Alain Jungo, Raphael Meier, Ekin Ermiş, Marcela Blatti-Moreno, Evelyn Herrmann, Roland Wiest, and Mauricio Reyes. On the effect of inter-observer variability for a reliable estimation of uncertainty of medical image segmentation. In *Medical Image Computing and Computer Assisted Interventions, MICCAI*, pages 682–690. Springer, 2018.
- [20] D Karimi, G Nir, L Fazli, P C Black, L Goldenberg, and S E Salcudean. Deep Learning-Based Gleason Grading of Prostate Cancer From Histopathology Images—Role of Multiscale Decision Aggregation and Data Augmentation. *IEEE Journal of Biomedical and Health Informatics*, 24(5):1413–1426, 2020. doi: 10.1109/JBHI.2019.2944643.
- [21] Alexander Kolesnikov, Xiaohua Zhai, and Lucas Beyer. Revisiting self-supervised visual representation learning. In *Proceedings of the IEEE conference on Computer Vision and Pattern Recognition*, pages 1920–1929, 2019.
- [22] Alex Krizhevsky, Geoffrey Hinton, and Others. Learning multiple layers of features from tiny images. Technical report, 2009.
- [23] Alex Krizhevsky, Ilya Sutskever, and Geoffrey E. Hinton. Imagenet classification with deep convolutional neural networks. In *Advances in neural information processing systems*, volume 60, pages 1097–1105. Association for Computing Machinery, 2012. doi: 10.1145/3065386.
- [24] S Kullback and R A Leibler. On Information and Sufficiency. *Ann. Math. Statist.*, 22(1):79–86, 1951. doi: 10.1214/aoms/1177729694.
- [25] Samuli Laine and Timo Aila. Temporal ensembling for semi-supervised learning. In *International Conference on Learning Representations*, 2017.
- [26] Daniel Langenkämper, Robin van Kevelaer, Autun Purser, and Tim W Nattkemper. Gear-Induced Concept Drift in Marine Images and Its Effect on Deep Learning Classification. *Frontiers in Marine Science*, 7, 2020. ISSN 2296-7745. doi: 10.3389/fmars.2020.00506.
- [27] Dong-Hyun Lee. Pseudo-label: The simple and efficient semi-supervised learning method for deep neural networks. In *Workshop on challenges in representation learning, ICML*, volume 3, page 2, 2013.
- [28] Junnan Li, Richard Socher, and Steven C. H. Hoi. DivideMix: Learning with Noisy Labels as Semi-supervised Learning. In *International Conference on Learning Representations*, pages 1–14, 2020.
- [29] Wen Li, Limin Wang, Wei Li, Eiríkur Agustsson, and Luc Van Gool. WebVision Database: Visual Learning and Understanding from Web Data. 2017.
- [30] Jeremiah Liu, Zi Lin, Shreyas Padhy, Dustin Tran, Tania Bedrax Weiss, and Balaji Lakshminarayanan. Simple and principled uncertainty estimation with deterministic deep learning via distance awareness. *Advances in Neural Information Processing Systems*, 33:7498–7512, 2020.
- [31] Sheng Liu, Jonathan Niles-Weed, Narges Razavian, and Carlos Fernandez-Granda. Early-Learning Regularization Prevents Memorization of Noisy Labels. *Advances in neural information processing systems*, 33:20331–20342, 2020.
- [32] Adam Marcu, Antonia; Prugel-Bennett. On Data-centric Myths. *NeurIPS 2021 Data-centric AI workshop*, 2021.
- [33] Mary L McHugh. Interrater reliability: the kappa statistic. *PubMed, Biochemia*(3):276–82, 2012.
- [34] Mohammad Motamedi, Nikolay Sakharnykh, and Tim Kaldewey. A Data-Centric Approach for Training Deep Neural Networks with Less Data. *NeurIPS 2021 Data-centric AI workshop*, 2021.
- [35] Kevin P Murphy. *Machine learning: a probabilistic perspective*. MIT press, 2012.

- [36] Zachary Nado, Neil Band, Mark Collier, Josip Djolonga, Michael W Dusenberry, Sebastian Farquhar, Angelos Filos, Marton Havasi, Rodolphe Jenatton, Ghassen Jerfel, and Others. Uncertainty Baselines: Benchmarks for uncertainty & robustness in deep learning. *arXiv preprint arXiv:2106.04015*, 2021.
- [37] Curtis G. Northcutt, Anish Athalye, and Jonas Mueller. Pervasive Label Errors in Test Sets Destabilize Machine Learning Benchmarks. *35th Conference on Neural Information Processing Systems (NeurIPS 2021) Track on Datasets and Benchmarks*, 2021.
- [38] Rafal Obuchowicz, Mariusz Oszust, and Adam Piorkowski. Interobserver variability in quality assessment of magnetic resonance images. *BMC Medical Imaging*, 20(1):109, 2020. ISSN 1471-2342. doi: 10.1186/s12880-020-00505-z.
- [39] E.A. A Ooms, H.M. M Zonderland, M.J.C. J C Eijkemans, M. Kriege, B. Mahdavian Delavary, C.W. W Burger, and A.C. C Ansink. Mammography: Interobserver variability in breast density assessment. *The Breast*, 16(6):568–576, 2007. ISSN 09609776. doi: 10.1016/j.breast.2007.04.007.
- [40] Adam Paszke, Sam Gross, Francisco Massa, Adam Lerer, James Bradbury, Gregory Chanan, Trevor Killeen, Zeming Lin, Natalia Gimelshein, Luca Antiga, Alban Desmaison, Andreas Kopf, Edward Yang, Zachary DeVito, Martin Raison, Alykhan Tejani, Sasank Chilamkurthy, Benoit Steiner, Lu Fang, Junjie Bai, and Soumith Chintala. PyTorch: An Imperative Style, High-Performance Deep Learning Library. In *Advances in Neural Information Processing Systems 32*, pages 8024–8035. Curran Associates, Inc., 2019.
- [41] Joshua Peterson, Ruairidh Battleday, Thomas Griffiths, and Olga Russakovsky. Human uncertainty makes classification more robust. *Proceedings of the IEEE International Conference on Computer Vision*, 2019-Octob:9616–9625, 2019. ISSN 15505499. doi: 10.1109/ICCV.2019.00971.
- [42] Monty Santarossa, Ayse Kilic, Claus von der Burchard, Lars Schmarje, Claudius Zelenka, Stefan Reinhold, Reinhard Koch, and Johann Roeder. MedRegNet: unsupervised multimodal retinal-image registration with GANs and ranking loss. In *Medical Imaging 2022: Image Processing*, volume 12032, pages 321–333. SPIE, 2022.
- [43] Lars Schmarje, Claudius Zelenka, Ulf Geisen, Claus-C. Glüer, and Reinhard Koch. 2D and 3D Segmentation of uncertain local collagen fiber orientations in SHG microscopy. *DAGM German Conference of Pattern Recognition*, 11824 LNCS(November):374–386, 2019. ISSN 23318422. doi: 10.1007/978-3-030-33676-9_26.
- [44] Lars Schmarje, Johannes Brünger, Monty Santarossa, Simon-Martin Schröder, Rainer Kiko, and Reinhard Koch. Fuzzy Overclustering: Semi-Supervised Classification of Fuzzy Labels with Overclustering and Inverse Cross-Entropy. *Sensors*, 21(19):6661, 2021. ISSN 1424-8220. doi: 10.3390/s21196661.
- [45] Lars Schmarje, Yuan-Hong Liao, and Reinhard Koch. A Data-Centric Image Classification Benchmark. *NeurIPS 2021 Data-centric AI workshop*, 2021.
- [46] Lars Schmarje, Monty Santarossa, Simon-Martin Schroder, Reinhard Koch, Simon-Martin Schröder, Reinhard Koch, Simon-Martin Schroder, and Reinhard Koch. A Survey on Semi-, Self-and Unsupervised Learning for Image Classification. *IEEE Access*, pages 1–1, 2021. ISSN 2169-3536. doi: 10.1109/ACCESS.2021.3084358.
- [47] Lars Schmarje, Monty Santarossa, Simon-Martin Schröder, Claudius Zelenka, Rainer Kiko, Jenny Stracke, Nina Volkmann, and Reinhard Koch. A data-centric approach for improving ambiguous labels with combined semi-supervised classification and clustering. *arXiv*, 2022.
- [48] T Schoening, A Purser, D Langenkämper, I Suck, J Taylor, D Cuvelier, L Lins, E Simon-Lledó, Y Marcon, D O B Jones, T Nattkemper, K Köser, M Zurowietz, J Greinert, and J Gomes-Pereira. Megafauna community assessment of polymetallic-nodule fields with cameras: platform and methodology comparison. *Biogeosciences*, 17(12):3115–3133, 2020. doi: 10.5194/bg-17-3115-2020.

- [49] Kihyuk Sohn, David Berthelot, Chun-Liang Li, Zizhao Zhang, Nicholas Carlini, Ekin D. Cubuk, Alex Kurakin, Han Zhang, and Colin Raffel. FixMatch: Simplifying Semi-Supervised Learning with Consistency and Confidence. *Advances in Neural Information Processing Systems 33 pre-proceedings (NeurIPS 2020)*, 2020.
- [50] Hwanjun Song, Minseok Kim, Dongmin Park, Yooju Shin, and Jae-Gil Lee. Learning From Noisy Labels With Deep Neural Networks: A Survey. *IEEE Transactions on Neural Networks and Learning Systems*, pages 1–19, 2022. ISSN 2162-237X. doi: 10.1109/TNNLS.2022.3152527.
- [51] Igor Stępień, Rafał Obuchowicz, Adam Piórkowski, and Mariusz Oszust. Fusion of Deep Convolutional Neural Networks for No-Reference Magnetic Resonance Image Quality Assessment. *Sensors*, 21(4), 2021. ISSN 1424-8220. doi: 10.3390/s21041043.
- [52] Antti Tarvainen and Harri Valpola. Mean teachers are better role models: Weight-averaged consistency targets improve semi-supervised deep learning results. In *ICLR*, 2017.
- [53] N Volkmann, J Brünger, J Stracke, C Zelenka, R Koch, N Kemper, and B Spindler. Learn to train: Improving training data for a neural network to detect pecking injuries in turkeys. *Animals* 2021, 11:1–13, 2021. doi: 10.3390/ani11092655.
- [54] Nina Volkmann, Johannes Brünger, Jenny Stracke, Claudius Zelenka, Reinhard Koch, Nicole Kemper, and Birgit Spindler. So much trouble in the herd: Detection of first signs of cannibalism in turkeys. In *Recent advances in animal welfare science VII Virtual UFAW Animal Welfare Conference*, page 82, 2020.
- [55] Jiaheng Wei, Zhaowei Zhu, Hao Cheng, Tongliang Liu, Gang Niu, and Yang Liu. Learning with Noisy Labels Revisited: A Study Using Real-World Human Annotations. 2021.
- [56] Sangdoo Yun, Seong Joon Oh, Byeongho Heo, Dongyoon Han, Junsuk Choe, and Sanghyuk Chun. Re-Labeling ImageNet: From Single to Multi-Labels, From Global to Localized Labels. In *Proceedings of the IEEE/CVF Conference on Computer Vision and Pattern Recognition (CVPR)*, pages 2340–2350, 2021.
- [57] Zizhao Zhang, Han Zhang, Sercan O. Arik, Honglak Lee, and Tomas Pfister. Distilling Effective Supervision from Severe Label Noise. *Conference on Computer Vision and Pattern Recognition*, 2020.